Proc. Indian Acad. Sci. (Chem. Sci.), Vol. 106, No. 7, December 1994, pp. 1595–1604.

Applications of high resolution magnetic resonance imaging (MRI) and spectroscopy (MRS) techniques to plant materials

N R JAGANNATHAN, R JAYASUNDAR, V GOVINDARAJU and P RAGHUNATHAN*

Department of Nuclear Magnetic Resonance, All India Institute of Medical Sciences, New Delhi 110029, India

Abstract. Magnetic resonance imaging (MRI) and *in vivo* magnetic resonance spectroscopic (MRS) techniques have been applied to a number of plant materials. The study demonstrates the usefulness of these methods in nondestructively estimating several factors related to pathology and histochemistry in important cash crops.

Keywords. Magnetic resonance imaging (MRI); *in vivo* magnetic resonance spectroscopy; plant materials.

1. Introduction

Proton magnetic resonance imaging (MRI) has become well established as an extensively used diagnostic tool in clinical radiology (Gadian 1982). The advantage of this method is that image information on 'soft' or 'mobile' protonic structures is available, often to an exquisite degree of detail, from the surface as well as from the interior of the examined objects without sample damage or destruction. The non-destructive nature of this method makes it an attractive option for studying a variety of biological materials. While magnetic resonance images map the spatial distribution of mobile nuclei (more specifically the protons), techniques of *in vivo* magnetic resonance spectroscopy (MRS) on localized image voxels can be used to obtain a good deal of information on water, lipid and carbohydrate distribution in many morphologically well-defined compartments of cash crops.

Applications of MRI and MRS techniques have, however, been very limited in studies of agricultural products such as fruits and vegetables (Lauterbur 1974; Mansfield and Pykett 1978; Connelly *et al* 1987; Ishida *et al* 1989, 1994; Duce *et al* 1992) and other plant systems (Bottomley *et al* 1986; Hall *et al* 1986; Johnson *et al* 1987; Pope *et al* 1991; Halloin *et al* 1993). In this paper, we present the MRI and MRS investigations carried out on some commonly used plant materials such as the papaya (*Carica papaya*), coconut (*Cocos nucifera*) and egg plant (*Solanum melongena*, which goes by the common name of 'brinjal' in India). Our objective is essentially to demonstrate the high degree of resolution and information content available in such studies, and thence to highlight the potential applications of such methods for

*For correspondence

noninvasively examining and improving cash crops, as well as for developing novel techniques of *in vivo* histochemical estimation in agricultural and plant sciences.

2. Methods

The imaging and spectroscopic experiments on coconut and papaya have been carried out at two different magnetic fields, using the 4·7 T Bruker Biospec and 1·5 T Siemens MRI/MRS spectrometers. Studies on brinjal and coconut were carried out at 4·7 T and 1·5 T, respectively. Multiple slice T_1- and T_2-weighted images have been recorded in transverse, coronal and sagittal planes using the standard spin echo sequence (Edelstein *et al* 1980). Localized *in vivo* spectroscopy has been carried out using STEAM (Frahm *et al* 1987) and PRESS (Bottomley 1987) RF pulse sequences. Careful magnetic field shimming at both the global (i.e. whole object) and voxel levels was performed for all the plant specimens prior to acquiring the proton magnetic resonance spectra with different echo times (TE = 135 or 270 ms) and a repetition time TR = 3 s. The time domain signals were Fourier-transformed after zero-filling and exponential multiplication. All the reported chemical shifts are related to TMS at zero ppm using water as an internal standard. The normal 1D NMR spectrum of coconut water was recorded at 400 MHz using a Bruker AMX 400 NMR spectrometer.

All the plant specimens used in this work were procured locally, and several randomly selected samples were studied on different days for each plant specimen.

3. Results and discussion

3.1 *Brinjal* (*Solanum melongena*)

The two morphological variants of the commonly available brinjal, the big bulbous species and the slender elongated variety, have been investigated. Typical T_1- and T_2-weighted images in the transverse, coronal and sagittal sections for the bulbous specimen are shown in figure 1. In the T_1-weighted image, contrast between the skin, vascular tissue and the seeds in the interior is sufficiently pronounced for easy identification, whereas in the T_2-weighted image only the seeds appear hyperintense. The hyperintensity (brightness) of the seeds in both the T_1- and T_2-weighted images (figures 1a, d) implies that the seeds have a shorter T_1 and a longer T_2 relaxation times. Another very interesting aspect is the characteristic distribution of the seeds in this species of brinjal which is totally absent in the elongated variety (vide infra). Moreover, the entire seed formation is concentrated in the core region, with practically no seeds appearing near the stem – see figures 1b, c.

T_1-weighted spin-echo images of coronal section of the elongated brinjal species are shown in figure 2. As is seen clearly, the image quality is the same as in the bulbous species in terms of contrast and resolution, except that the seeds are not distributed according to any recognizable pattern. The figure also demonstrates the image of an elongated brinjal that has deteriorated due to fungal growth. The decayed portion is very clearly seen. Visualization of such changes induced in the interior of the vegetables due to fungal growth and other forms of tissue decay by means of

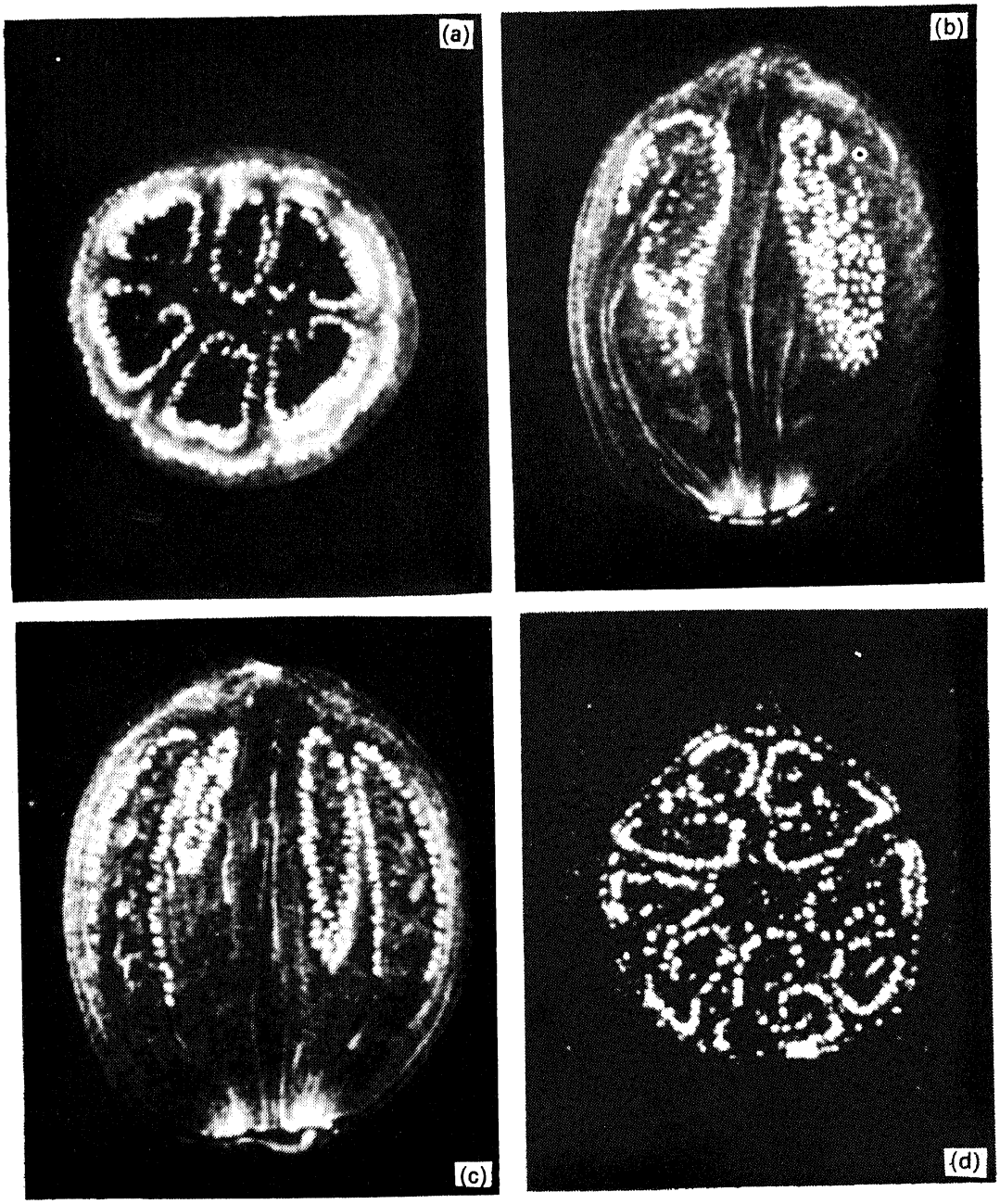

Figure 1. T_1-weighted spin echo images of big bulbous brinjal in the (**a**) transverse, (**b**) coronal and (**c**) sagittal sections with TR = 600 ms, TE = 19·1 ms and slice thickness = 3 mm. (**d**) corresponds to the T_2-weighted image of the transverse section with TR = 2500 ms and TE = 70 ms.

nondestructive MRI scanning should find obvious applications in the agricultural industry and in research.

Owing to the observation of considerably broadened proton resonances and T_2 values, typically around 3 to 5 ms, in the brinjal specimens, further localized *in vivo* MRS investigations have not been carried out.

Figure 2. T_1-weighted images of 3 mm coronal section of the slender elongated brinjal: (**a**) normal and (**b**) spoilt.

3.2 *Coconut (Cocos nucifera)*

Two groups of coconut, namely, the tender and the mature (ripe) ones, have been investigated. The T_1- and T_2-weighted images acquired for these specimens at 1·5 T are shown in figure 3.

In the tender coconut (images not shown) water dominates, whereas in the ripened species a pulp of about 1·5 cm thickness plus the inner core water is clearly depicted. The following additional morphological details are of potential diagnostic value.

In the T_1-weighted image (figure 3a) the pulp appears hyperintense and the water relatively darker. The interfacial pulp layer close to the water is isointense with the water, whereas in the T_2-weighted image (figure 3b) the pulp appears darker, with the water and the pulp-water boundary showing up brighter. The reason for the darker appearance of the pulp on T_2-weighting is attributable to the fact that the fat constituting the pulp has a shorter T_2 value.

Transverse and coronal T_1-weighted images of a normal coconut at 4·7 T are shown in figure 4. This coconut developed a crack on the inner shell as well as in the pulp and the images were recorded on different days. These are shown in figure 5. Due to the crack the coconut became progressively more rancid, and the dark spots on the images in coconut water are due to fungal development.

The major chemical constituents of coconut water are sugars and minerals while the minor ones are fat and nitrogenous substances such as amino acids. The pleasant taste is due to sugar and mineral matter. Minor constituents such as fat, free amino acids, nucleic acids, organic acids and dissolved gases also contribute to the overall flavour and taste (Jayaleshmy *et al* 1986).

Figure 6 shows the *in vivo* localized water suppressed proton NMR spectra (0 to

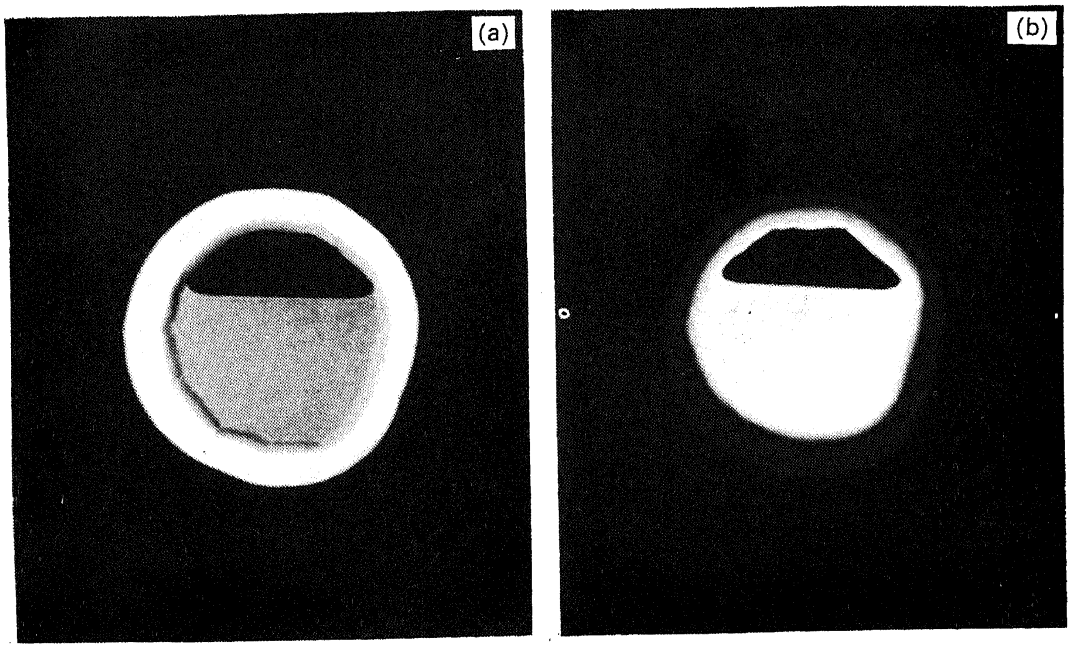

Figure 3. 5 mm transverse section images of mature coconut at 1·5 T. (**a**) T_1-weighted with TR = 520 ms and TE = 15 ms, and (**b**) T_2-weighted with TR = 2500 ms and TE = 90 ms.

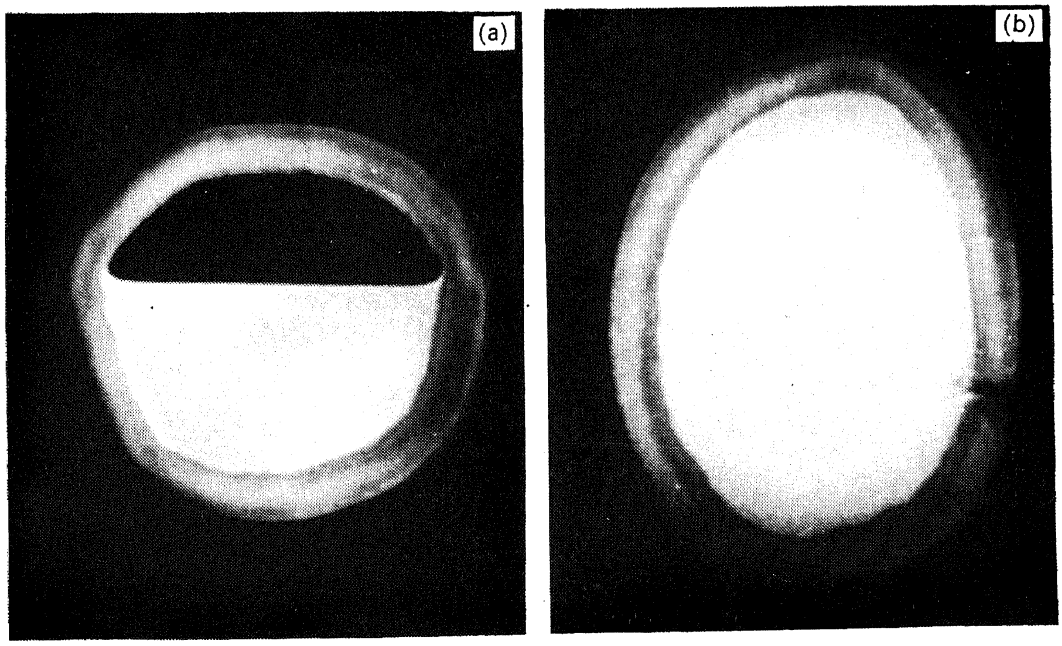

Figure 4. T_1-weighted images of normal mature coconut at 4·7 T, with TR = 800 ms, TE = 19·1 ms and slice thickness = 4 mm: (**a**) transverse and (**b**) coronal.

4·2 ppm range) of water from a tender and a mature coconut, with an 8 cm^3 voxel at 1·5 T. From figure 6a it is clear that the mature coconut water contains resonances from sugars at 3·5 ppm and lipids at 1·1 ppm, respectively, whereas in the tender coconut there is no lipid peak. However, some additional resonances in the sugar region are observed in the tender coconut (figure 6b). This could be due to the variation in the chemical constituents between the various specimens of coconut,

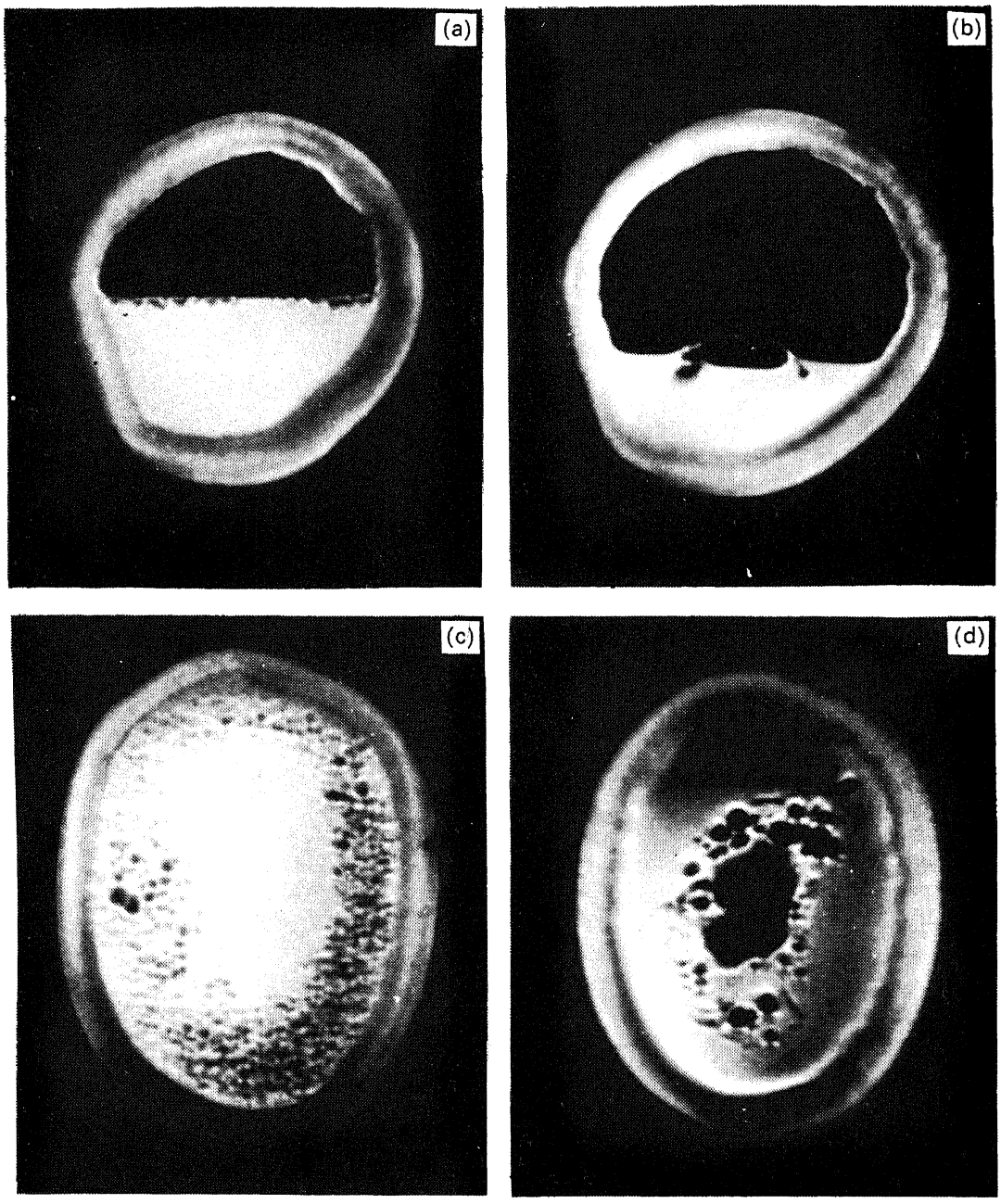

Figure 5. T_1-weighted images of rancid mature coconut at 4·7 T recorded after 1 week (**a, c**) and 4 weeks (**b, d**), with the same experimental parameters as given in figure 4. (a) and (b): transverse; (c) and (d): coronal.

arising at different stages of maturation. We are presently analysing these aspects further.

Figure 7 shows the *in vitro* proton NMR spectrum of water from a mature coconut at 9·4 T with water suppression. It is interesting to notice the gross similarity between this spectrum and that recorded at 1·5 T. As expected, the resonances are all highly resolved especially in the sugar region. In addition, the peak near 1·5 ppm may be assigned to the protons of methyls arising from $CH_3-C=$ groups. The 5·1 to 5·5 ppm region could be due to protons present in groups such as $H_2C=$, $HC=$, $HC-O-$.

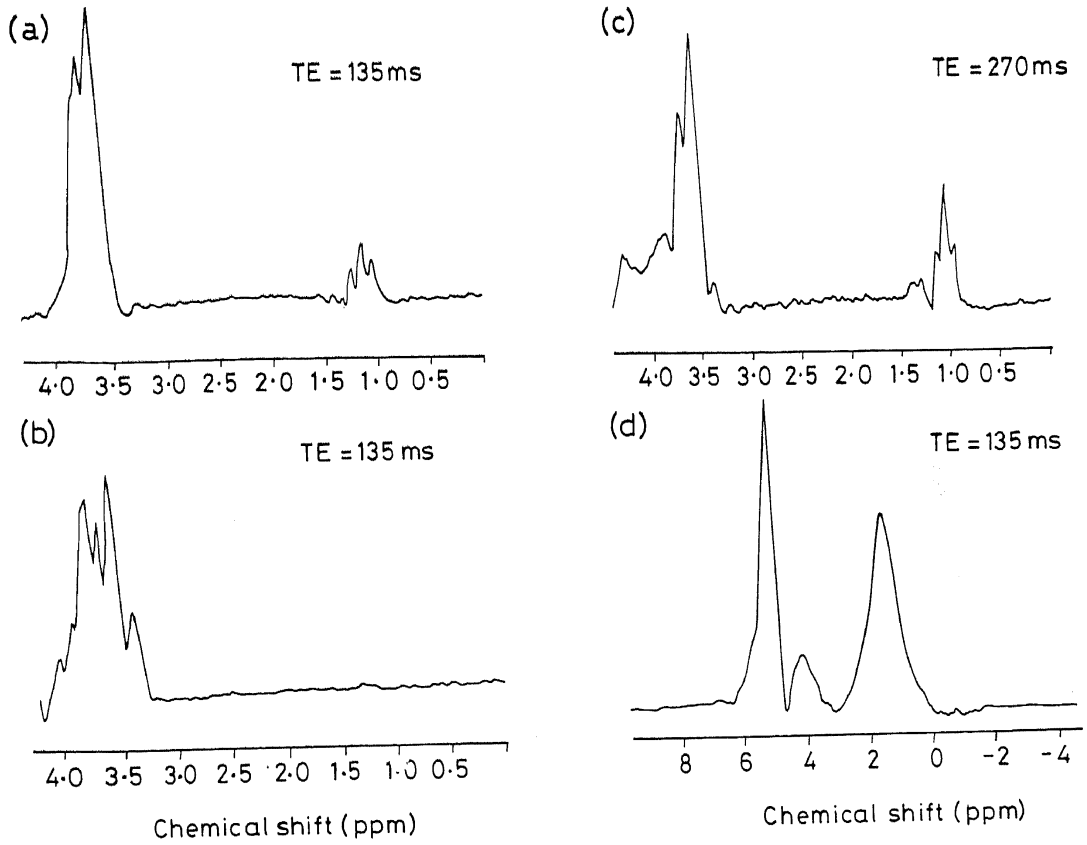

Figure 6. 1·5 T *in vivo* water suppressed proton NMR spectra of ($20 \times 20 \times 20\,mm^3$) voxel localized in: (**a**) and (**c**) water from mature coconut, (**b**) water from tender coconut and (**d**) pulp from mature coconut.

Other minor resonances appearing in the spectrum of figure 7 have not been assigned.

Figure 8 shows *in vivo* proton NMR spectrum of water from a mature rancid coconut at 4·7 T. From the spectrum, it is clear that many field resonances are absent except for the small contribution from sugar resonances around 3·4 ppm. The absence of lipid methyls around 1·1 ppm and other resonances could be due to the fact that the fungus may have used this up for its growth (Halloin *et al* 1993).

As exemplified above, the ability to monitor visually and nondestructively the degradation of coconut by means of MRI and MRS and other vegetables will be of much use in agricultural industry for quality control as well as for evaluating the extent and nature of bacterial and fungal growth. The observance of numerous resonances due to a variety of chemicals present in these systems could also provide useful information about their pathology and histochemistry.

3.3 *Papaya (Carica papaya)*

Papaya is a very common fruit in most parts of India and is often included in the diet. The fruit is known to contain mainly water and small quantities of a number of vitamins and proteins and hence would be a good system to be studied by MRI/MRS technique to map out the distribution of water protons as well as to identify the number of chemicals present in the edible pulp. While a more extended

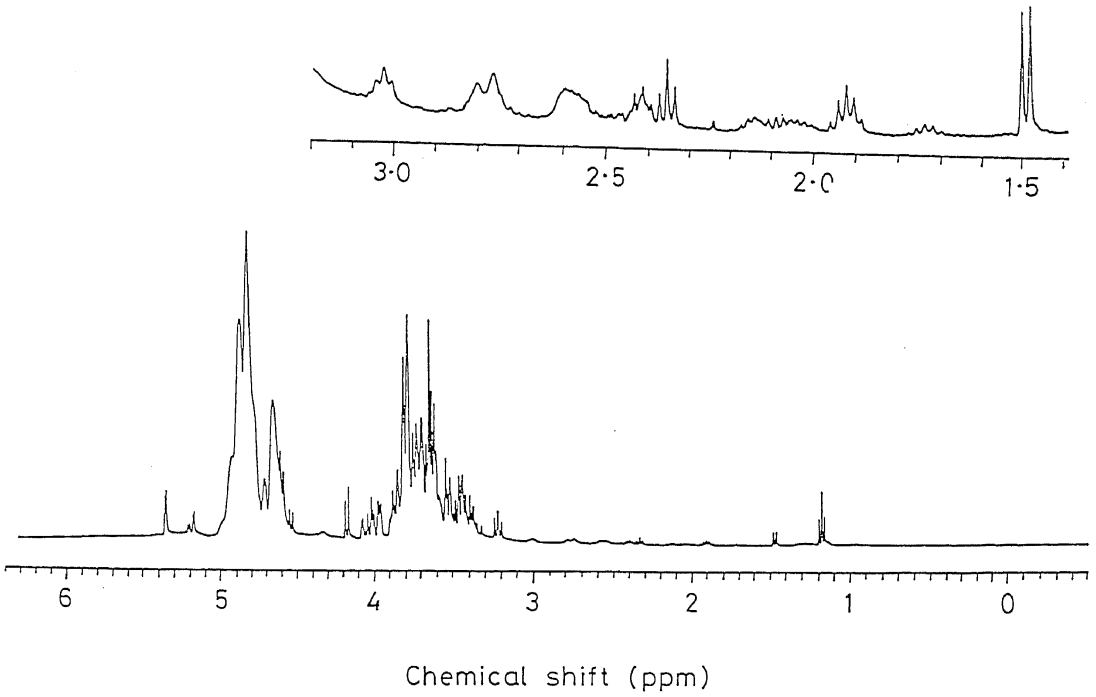

Figure 7. *In vitro* proton NMR spectrum of water from mature coconut at 9·4 T.

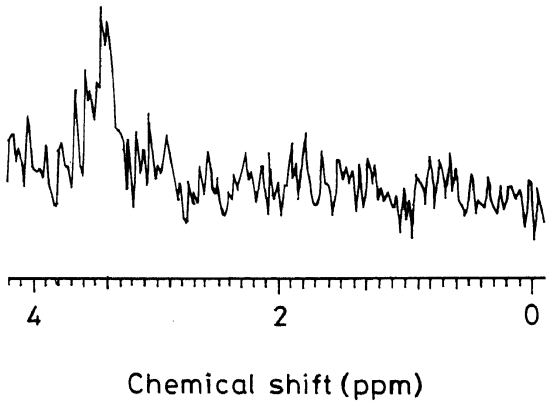

Figure 8. 4·7 T *in vivo* proton NMR spectrum from ($15 \times 15 \times 15\,mm^3$) voxel localized in water from rancid mature coconut.

investigation based on the technique of chemical shift imaging (Pope *et al* 1991) is already under way in our laboratory, we present here some salient MRI results.

Figure 9 shows T_1-weighted images of ripe papaya in the transverse, coronal and sagittal planes. One notices that there is polydispersity in the seed size. Furthermore, as is evidenced by the contrast, a small percentage of the seeds seems to contain more mobile protons which are isointense with the protons of the pulp. It is seen from the coronal (figure 9b) and sagittal (figure 9c) sections that the seeds are concentrated preferentially in the centre and at the end region away from the stem.

Figure 10 compares the transverse T_1- and T_2-weighted images of a slice characterized by a concentration of seeds. Clearly, the pulp appears darker in the T_2-weighted image (figure 10b), whereas the seeds appear brighter in the two differently weighted

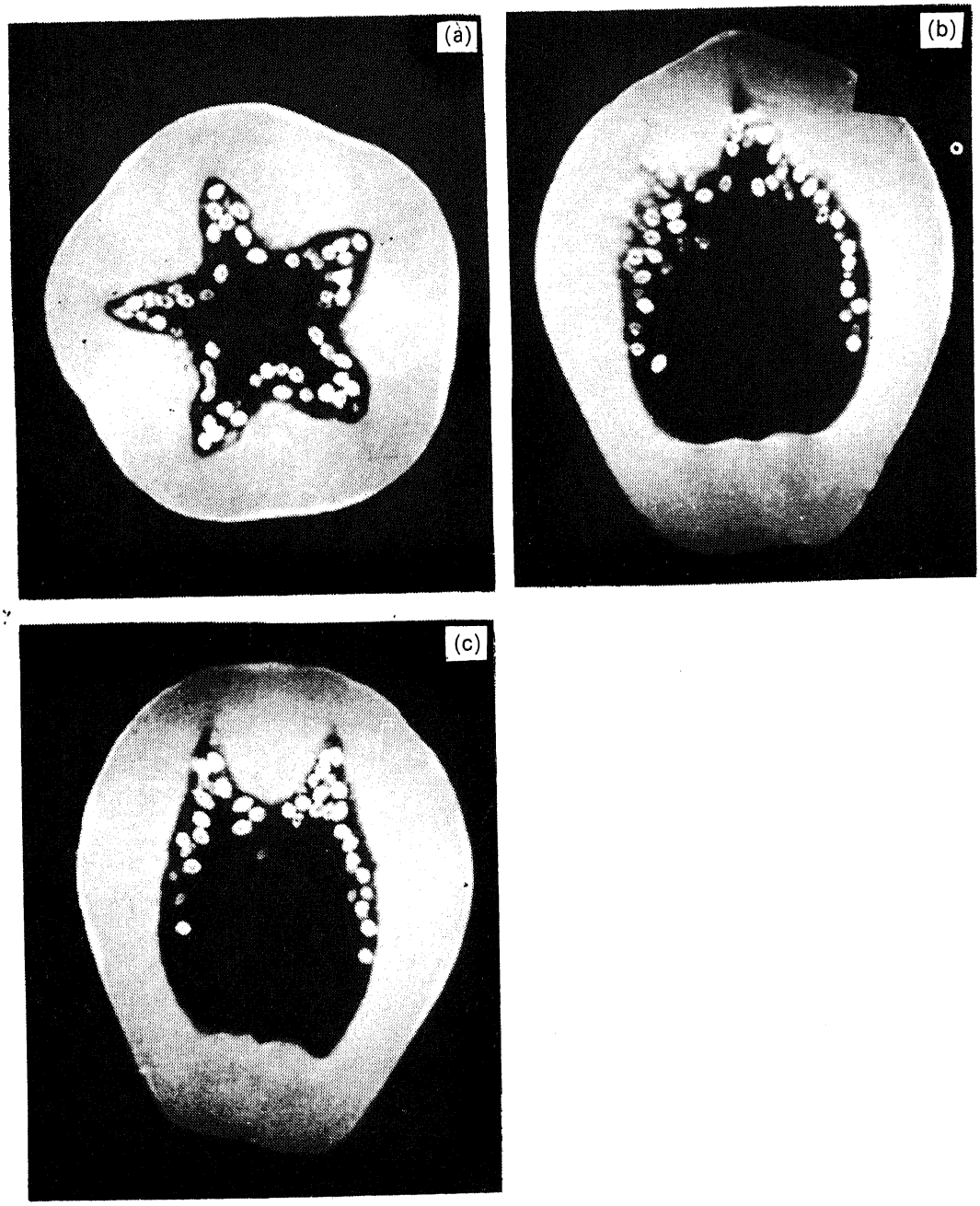

Figure 9. T_1-weighted images of papaya with TR = 520 ms, TE = 15 ms and slice thickness = 5 mm: (**a**) transverse (**b**) coronal and (**c**) sagittal.

images. This pattern is analogous to that observed for the bigger variety of brinjal discussed earlier.

4. Conclusion

The representative examples cited above serve to demonstrate the potential of modern MRI and MRS methodologies in nondestructive estimation of factors related to pathology and histochemistry in important cash crops. Suitably T_1- and T_2-

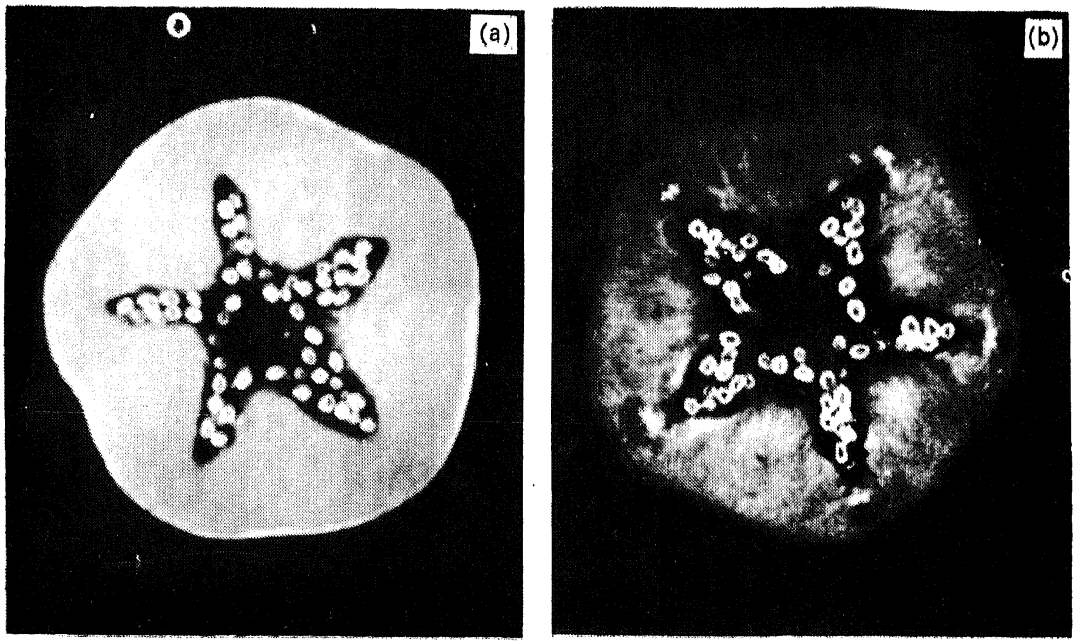

Figure 10. Images of the 5 mm transverse section of papaya (**a**) T_1-weighted with TR = 520 ms and TE = 15 ms, (**b**) T_2-weighted with TR = 2500 ms and TE = 90 ms.

discriminated images at various growth stages of the plants together with localized MRS techniques could even lead to quantitative assessments of metabolite concentrations. Several further studies are currently in progress in our laboratory.

Acknowledgement

Generous financial assistance from the Departments of Science and Technology and Biotechnology, New Delhi is gratefully acknowledged. The spectrum shown in figure 7 was recorded on the AMX 400 MHz NMR spectrometer available at the Sophisticated Instruments Facility, Indian Institute of Science, Bangalore.

References

Bottomley P A 1987 *Ann. New York Acad. Sci.* **508** 333
Bottomley P A, Rogers H H and Foster T H 1986 *Proc. Natl. Acad. Sci. USA* **83** 87
Connelly A, Lohman J A B and Loughman B C 1987 *J. Exp. Botany* **38** 1713
Duce S L, Carpenter T A, Hall L D and Hills B P 1992 *Magn. Reson. Imaging* **10** 289
Edelstein W A, Hutchinson J M S, Johnson G and Redpath G 1980 *Phys. Med. Biol.* **25** 751
Frahm J, Merboldt K D and Hanicke W 1987 *J. Magn. Reson.* **72** 502
Gadian D G 1982 *NMR and its application to living systems* (Oxford: Clarendon)
Hall L D, Rajanayagam V, Stewart W A and Steiner P R 1986 *Can. J. For. Res.* **16** 423
Halloin J M, Cooper T G, Potchem E J and Thompson T E 1993 *J. Am. Oil Chem. Soc.* **70** 1259
Ishida N, Kobayashi T, Koizumi M and Kano H 1989 *Agri. Biol. Chem.* **53** 2363
Ishida N, Koizumi M and Kano H 1994 *Scientia Horticulturae (Amsterdam)* **57** 335
Jayaleshmy A, Arumugham C, Narayanan C S and Mathew A G 1986 *J. Food Sci. Tech.* **23** 203
Johnson G A, Brown J M and Kramer P J 1987 *Proc. Natl. Acad. Sci. USA* **84** 2752
Lauterbur P C 1974 *Pure Appl. Chem.* **40** 149
Mansfield P and Pykett L 1978 *J. Magn. Reson.* **29** 355
Pope J M, Rumpel H, Kuhn W, Walker R, Leach D and Sarafis V 1991 *Magn. Reson. Imaging* **9** 357